Comparative studies of pelagic microbial methane oxidation within the redox zones of the Gotland Deep and Landsort Deep (central Baltic Sea)

G. Jakobs*, G. Rehder, G. Jost, K. Kießlich, M. Labrenz, and O. Schmale

Leibniz Institute for Baltic Sea Research Warnemünde (IOW), Rostock, Germany

*Correspondence to: Gunnar Jakobs (gunnar.jakobs@io-warnemuende.de)

Abstract

Pelagic methane oxidation was investigated in dependence on differing hydrographic conditions within the redox zone of the Gotland Deep (GD) and Landsort Deep (LD), central Baltic Sea. The redox zone of both deeps, which indicates the transition between oxic and anoxic conditions, was characterized by a pronounced methane concentration gradient between the deep water (GD: 1233 nM, 223 m; LD: 2935 nM, 422 m) and the surface water (GD and LD < 10 nM). This gradient together with a ^{13}C CH_4 enrichment ($\delta^{13}C$ CH_4 deep water: GD -84 ‰, LD -71 ‰; redox zone: GD -60 ‰, LD -20 ‰; surface water: GD -47 ‰, LD -50 ‰; $\delta^{13}C$ CH_4 vs. Vienna Pee Dee Belemnite standard), clearly indicating microbial methane consumption within the redox zone. Expression analysis of the methane monooxygenase identified one active type I methanotrophic bacterium in both redox zones. In contrast, the turnover of methane within the redox zones showed strong differences between the two basins (GD: max. 0.12 nM d^{-1} and LD: max. 0.61 nM d^{-1}), with a nearly four times lower turnover time of methane in the LD (GD: 455 d, LD: 127 d). Vertical mixing rates for both deeps were calculated on the base of the methane concentration profile and the consumption of methane in the redox zone (GD: $2.5*10^{-6}$ m^2 s^{-1}, LD: $1.6*10^{-5}$ m^2 s^{-1}). Our study identified vertical transport of methane from the deep water body towards the redox zone as well as differing hydrographic conditions (lateral intrusions and vertical mixing) within the redox zone of these deeps as major factors that determine the pelagic methane oxidation.

1 Introduction

Methane is an atmospheric trace gas that influences the climate and the atmospheric chemistry (Wuebbles and Hayhoe, 2002). It is generated in terrestrial, limnic and marine ecosystems by biotic (Segers, 1998; Reeburgh, 2007) and abiotic mechanisms (Berndt et al., 1996; Keir et al., 2008). Although methane is trapped in aquatic sediments in vast amounts, marine environments only represent a negligible source for atmospheric methane (Reeburgh, 2007). In the marine system, microbial methane oxidation provides a control mechanism on the release of methane into the atmosphere (Bange et al., 1994; Valentine et al., 2001; Reeburgh, 2007; Schmale et al., 2012). Environmental studies regarding microbially mediated methane oxidation have been carried out for various aquatic systems. From marine water column studies it is known that methane is oxidized in the aerobic environment by MOB of type I, II and X, whereas in the anoxic waters this process is mediated by ANME I and II (Durisch-Kaiser et al., 2005; Schubert et al., 2006b; Blumenberg et al., 2007). Different electron acceptors are used for the consumption of methane (Modin et al., 2007; Knittel and Boetius, 2009). In the sediments, oxidation processes have been proven by oxygen, sulfate, nitrate, nitrite, iron and manganese, in the water column only by sulfate and oxygen (Reeburgh, 2007; Beal et al., 2009; Ettwig et al., 2010). According to their carbon assimilation that can either be performed by the ribulosemonophosphate (RuMP) or serine pathway, the aerobic methanotrophic bacteria (MOB) are separated into the main groups type I and type II, respectively. The thermophilic MOB type X represent a subgroup of type I and are capable to fix methane as well as carbon dioxide. Aerobic methanotrophs are able to oxidize methane via oxygen due to the key enzyme methane monooxygenase (MMO), which catalyzes the formation of methanol during the first step of methane oxidation. Only the particulate form of this enzyme (pMMO) is present in all three groups. The functional *pmoA* gene encoding the alpha subunit of pMMO is used as marker to identify methanotrophs in different

environments (Bourne et al., 2001; McDonald et al., 2008). The anaerobic oxidation of methane (AOM) via sulfate takes place by a consortium of methanotrophic archaea (ANME I, II and III) and sulfate reducing bacteria with a very low energy yield of ΔG^0 = -16.6 kJ/mol CH_4 compared to the energy yield of ΔG^0 = -773 kJ/mol CH_4 obtained by the aerobic oxidation of methane (Boetius et al., 2000; Valentine and Reeburgh, 2000). Methanotrophic archaea harbor the methyl coenzyme M reductase (MCR) that is also present in methanogenic archaea to catalyze the formation of methane (Hallam et al., 2003).

The bottom topography of the Baltic Sea consists of a series of sub-basins that are separated by narrow sills, which hamper the continuous water exchange with the North Sea. The hydrographic situation of the Baltic Sea is characterized by a freshwater discharge from the rivers and episodic inflows of saline water from the North Sea (estuarine circulation), Lass and Matthäus (2008). Ventilation of the deep water by saline oxygenated water from the North Sea (so-called Major Baltic Inflows) occurred irregularly over the last decades leading to long periods of deep water stagnation in the central Baltic Sea (Matthäus et al., 2008; Reissmann et al., 2009); the last Major Baltic Inflow took place in year 2003. The more frequent but less intense inflows contain water masses with a density too low to displace the old stagnant water in the deep basins and propagate laterally into intermediate water layers of the central Baltic Sea (Matthäus et al., 2008).

In the central and southern Baltic Sea the less saline surface and more saline deep water cause the formation of a permanent density boundary, the halocline, which has a crucial effect on the vertical exchange of matter and the renewal of deep water (Reissmann et al., 2009). Especially the downward diffusion of oxygen is affected by this density boundary leading to a vertical biogeochemical zonation with oxygen-limiting conditions in the intermediate and deep water body and the microbial turnover of organic matter by sulfate reduction or denitrification for example (Lass and Matthäus, 2008). The oxygenated surface water and the

anoxic deep water are separated by the redox zone. This zone is a smooth transition between oxic and anoxic conditions with an overlap of oxygen and hydrogen sulfide containing waters (Nausch et al., 2008; Labrenz et al., 2010; Dellwig et al., 2012). The pronounced chemical gradients in redox zones of stratified water columns are known to provide favorable conditions for different microbial processes such as ammonia oxidation, denitrification or methane oxidation (Brettar and Rheinheimer, 1992; Schubert et al., 2006a; Labrenz et al., 2010).

In the Gotland Basins, comprehensive water column investigations revealed a widespread release of methane from the sediments with strong methane enrichments in the stagnant anoxic water bodies (eastern Gotland Basin (Gotland Deep) and western Gotland Basin (Landsort Deep); max. 504 nM and 1086 nM, respectively; Schmale et al., 2010). Compared to the atmospheric equilibrium only slightly elevated methane concentrations (3 – 5 nM CH_4) prevail in the surface waters (Bange et al., 1994; Schmale et al., 2010; Gülzow et al., 2012). High resolution gas chemistry studies in the water column of the Gotland Basins showed a pronounced methane gradient and an enrichment of ^{13}C CH_4 within the pelagic redox zone that indicates microbial activity related to the aerobic oxidation of methane in that water depth (Schmale et al., 2012). This finding is supported by earlier methane oxidation rate measurements indicating that methane is preferentially oxidized under low oxygen concentrations (16 to 63 µM O_2; Dzyuban et al., 1999). Schmale et al. (2012) also showed that aerobic methane oxidation within the pelagic redox zone of the Gotland Deep is performed by members of type I methanotrophic bacteria. Furthermore, biomarker analysis could identify specific bacteriohopanepolyols (BHP) and phospholipid fatty acids (PLFA) that are characteristic for the presence of active type I methanotrophic bacteria (Berndmeyer et al., 2013).

Although microbial oxidation of methane in the water column represents an important sink of methane, the impact of dynamic environmental conditions like methane source strength and hydrodynamic forces on the efficiency of that mechanism is still insufficiently described (Reeburgh, 2007; Schmale et al., 2012). With its distinct oxic and anoxic stratified zones that are episodically perturbed by oceanographic events, the Baltic Sea provides an ideal field to investigate these effects on the methane cycle. In this study we focus on the influence of different hydrographic conditions (lateral intrusions and vertical mixing) on the methane turnover within the pelagic redox zone. For this scope, comparative interdisciplinary studies were carried out in the Gotland Deep and Landsort Deep. The combined data on methane chemistry, methane oxidation rates and molecular biological analysis will gain first insights into the temporal stability and regional transferability of microbial processes related to pelagic microbial methane consumption in the central Baltic Sea.

2 Study area

Investigations were carried out in the water column of the Gotland Deep (57°19.2‘N 20°03.0‘E, water depth 223 m) and Landsort Deep (58°35.0‘N 18°14.0‘E, water depth 422 m) located in the central Baltic Sea (Figure 1). Both sampling sites are characterized by different basin structures and hydrographic conditions (see section through the central Baltic Sea, Figure 1C). The Landsort Deep represents the deepest areal in the western Gotland Basin (max. depth 460 m) with a relatively small spatial dimension. In contrast, the eastern Gotland Basin represents the largest basin of the Baltic Sea with a maximum water depth of about 250 m at the Gotland Deep.

During an inflow of saline waters from the North Sea towards the central Baltic Sea, this water mass propagates first into the eastern Gotland Basin. Depending on the strength of the inflow, the deep water mass can continue its path via a northern passage towards the western

Gotland Basin. The travel of inflowing saline water from the North Sea along different basins and sills promotes the mixing between saline bottom water and less saline overlying water masses, resulting in a decreasing salt content of the intruding water along its way into the central Baltic Sea. Accordingly, the Landsort Deep is characterized by less frequent and weaker lateral intrusions, resulting in a more stable oxic/anoxic transition zone (redox zone) and a lower deep water salinity compared to the Gotland Deep (Matthäus et al., 2008).

3 Materials and Methods

3.1 Sampling strategy

Samples were taken during cruise 06EZ/12/13 on RV Elisabeth Mann Borgese in July/August 2012. Sampling for molecular biological analysis and radiotracer experiments were performed after first inspection of the physical parameters of the water column (e.g. salinity, turbidity) using a CTD probe (CTD system Seabird sbe911+ and a turbidity sensor ECO FLNTU, WET Labs) and methane concentration analysis on board to identify the most relevant depths intervals for methane oxidation. To obtain enough sample volume for all analysis water samples were taken within five casts on two consecutive days at each sampling site. Methane, oxygen and hydrogen sulfide analysis were performed on the first day of sampling. Water samples for determination of methane oxidation rates and molecular biological analysis were obtained on the following day. Between these two samplings the physical parameters of the water column showed no significant differences.

3.2 Gas analysis

3.2.1 Methane, oxygen and hydrogen sulfide

For the determination of methane concentrations, water samples were transferred from the rosette water sampler into 250 ml glass flasks, and poisoned with 500 µl saturated mercury chloride solution. Methane concentrations were determined directly after the cruise using a modified purge & trap procedure (Michaelis et al., 1990; Thomas, 2011). This modified method includes following process steps: the samples were stripped with helium to remove volatile constituents (purge step), dried using a Nafion® trap (Perma Pure LLC., USA), cryofocussed at -120°C (ethanol/nitrogen) on HayeSep D® (Valco Instruments Company Inc., Switzerland) desorbed by heating at 85°C, and analyzed using a gas chromatograph (Shimadzu GC-2014) equipped with a flame ionization detector. The concentration of oxygen was determined by titration method (precision ± 0.9 µM O_2) and the hydrogen sulfide concentrations were measured calorimetrically using the methylene blue method (precision ± 1.0 µM H_2S) (Grasshoff et al., 1999). Oxygen concentrations were only determined for samples virtually devoid of hydrogen sulfide.

3.2.2 Stable carbon isotope ratio of methane

Gas samples for stable carbon isotope analysis of methane ($\delta^{13}C$ CH_4) were gained using a vacuum degassing system described in Keir et al. (2009) in detail. Following this method, a water sample of 600 ml was transferred into a 1100 ml pre-evacuated glass bottle leading to a partial degassing of the water sample. The extracted gas was decompressed to atmospheric pressure and subsequently transferred to a gastight burette. An aliquot of the extracted gas was conserved in a 10 ml pre-evacuated glass crimp vial containing a saturated sodium chloride solution poisoned with mercury chloride. The isotope ratio was determined using an isotope-ratio mass spectrometer (MAT 253, Thermo Electron, Germany) according to the method described by Schmale et al. (2012). $\delta^{13}C$ CH_4 values are expressed versus VPDB (Vienna Pee Dee Belemnite) standard.

3.3 Methane oxidation rates

3.3.1 Sampling and $^{14}CH_4$ tracer preparation

Immediately before sampling the sample bottles were flushed with argon. According to the sampling procedure by Reeburgh et al. (1991) water samples were directly transferred from the rosette sampler into transfusion bottles and sealed air-free with aluminum screw caps and natural rubber septa. Three times the volume of the sample bottle (600 ml) was filled into the bottle in overflow, to avoid any entry of oxygen into the water samples. In contrast to methods described by Reeburgh et al. (1991) and Durisch-Kaiser et al. (2005) a larger sample volume (600 ml) was chosen, to account for the low specific $^{14}CH_4$ tracer activity ($^{14}CH_4$ dissolved in sterile anoxic water, injection volume 100 µl, activity 3 kBq) used in this procedure and to obtain sufficient labeled oxidation products even in case of a low methane turnover. The $^{14}CH_4$ activity of the injected tracer was determined by stripping of the tracer liquid with synthetic air and a following combustion step on a Cu(II)-oxide catalyst at 850°C (Treude et al., 2003). The resulting $^{14}CO_2$ was trapped with a mixture of phenylethylamine and ethyleneglycolmonomethylether (1:7 v/v), and the activity was measured by liquid scintillation counting. The final concentration of the injected tracer (each sample labeled with 5 nM $^{14}CH_4$) was lower than the *in situ* methane concentrations of the water samples to prevent any artificial stimulation of microbial methane oxidation by increased methane concentrations.

3.3.2 Sample processing

After tracer injection, the bottles were incubated in the dark for 3 days near *in situ* temperature (~ 4 °C). The microbial activity was terminated by injection of sodium hydroxide

(500 µl, 50 % (w/w)) which led to the precipitation of dissolved inorganic carbon compounds ($CO_{2(aq)}$, HCO_3^-, CO_3^{2-}). For trapping of the microbial formed $^{14}CO_2$ a method described by Treude et al. (2005) was used. Briefly, the samples were transferred in gastight bottles equipped with scintillation vials positioned in the gas headspace below the bottle cap. These vials contained a mixture of sodium hydroxide (2.5 % w/w) and phenylethylamine in equal amounts to capture the $^{14}CO_2$ released from the sample after acidification with hydrochloric acid (5 ml, 25 %) under stirring for 24 hrs. The activity of the scintillation vials was measured on a Tri-Carb 2910 TR (Perkin Elmer Inc., USA) liquid scintillation counter using a scintillation cocktail (Irga-safe Plus, Perkin Elmer). For selected water depths incubation experiments were performed in triplicates to determine the standard deviation (*s* in percentage of the average, $n = 3$) of the measured oxidation rates for the upper oxic-, deep anoxic-, and oxic/anoxic transition zone in intermediate water depth (80 – 145 m). For the Gotland Deep, the standard deviation for the oxic zone is 12.4 %, the oxic/anoxic transition zone 8.8 % and the anoxic zone 134.4 % derived from triplicates sampled in 70, 85 and 175 m water depth, respectively. For the Landsort Deep, the standard deviation for the oxic zone is 11.7 %, oxic/anoxic transition zone 11.2 % and the anoxic zone 173.2 % determined by triplicates sampled in 70, 80 and 175 m water depth, respectively. Blank values were obtained by terminating with sodium hydroxide immediately after tracer addition and sample treatment as described above. Assuming a first-order kinetic during methane degradation, the methane oxidation rates (r_{ox}) were calculated according to Eq. (1),

$$r_{ox} = \frac{^{14}CO_2 * CH_4}{^{14}CH_4 * t * 0.9} \quad \left[nM\ d^{-1}\right] \tag{1}$$

where $^{14}CO_2$ is the radioactivity [dpm = disintegrations per minute] of the microbial formed carbon dioxide, $^{14}CH_4$ is the radioactivity [dpm] of the injected tracer, CH_4 is the *in situ* methane concentration of the water sample [nmol/l], t is the incubation time [d] and 0.9 the experimentally determined recovery factor (recovery factor of 1 indicates a quantitative release and capture of $^{14}CO_2$ produced by the turnover of CH_4). This factor was determined by a known amount of $H^{14}CO_3^-$ dissolved in water, followed by acidification, and the capture of $^{14}CO_2$ as described above. The turnover rate constant (k) in Eq. (2) expresses the fraction of $^{14}CH_4$ that is oxidized per unit time, whereby the turnover time of methane is represented by its reciprocal ($1/k$).

$$k = \frac{^{14}CO_2}{^{14}CH_4 * t * 0.9} \quad \left[d^{-1}\right] \tag{2}$$

Integrated methane oxidation rates (ir_{ox}) were calculated according to the trapezoid-rule displayed in Eq. (3). Therefore we subdivided the redox zone in depth intervals. Each depth interval was defined by two consecutive sampling depths, whereas dz [m] is the vertical distance between the two samples. $f(z)$ and $f(z+dz)$ are the corresponding oxidation rates (r_{ox}) [µmol d^{-1} m^{-3}] for each sampling depth. The total oxidation rate within the redox zone (ir_{ox}) was obtained by summing up the individual oxidation rates of each depth interval.

$$ir_{ox} = \frac{1}{2}\left(f(z) + f(z+dz)\right)dz \quad \left[\mu mol\, d^{-1}\, m^{-2}\right] \tag{3}$$

3.4 *pmoA* gene and transcript analysis

1000 ml of each sample were filtered on a Durapore filter (0.2 µm pore size, GVWP, Merck Millipore, USA), frozen in liquid nitrogen and stored at -80°C. DNA and RNA were extracted from frozen filters as described by Weinbauer et al. (2002). *pmoA* transcripts were analyzed with reverse transcriptase-PCR (30-33 cycles) using the primer system A189f/mb661r (Holmes et al., 1995; Costello and Lidstrom, 1999) followed by DGGE fingerprinting as described in Schmale et al. (2012). Visible bands were cut out of the gel, reamplified and sequenced by LGC Genomics GmbH (Berlin, Germany). Sequences were checked for quality using SeqMan software (DNASTAR Inc., USA). Phylogenetic affiliations of the partial sequences were initially estimated with the program BLAST (Altschul et al., 1990). In addition 50 ng DNA of each water sample was processed via PCR (30-35 cycles) and DGGE under the same conditions to determine the total methanotrophic assemblages within the entire water column.

4 Results

4.1 Gotland Deep

During our field study the temperature and salinity profiles (Figure 2A) demonstrated strong vertical gradients, revealing thermohaline stratification with pronounced density differences of individual water bodies. The thermocline extended from 15 to 30 m water depth and the halocline was located in a depth interval from 60 to 80 m. The vertical turbidity profile showed two maxima, one in the surface water and the other in around 127 m water depth. According to the content of oxygen (O_2, Figure 2B), the water column can be separated into different depths intervals (Tyson and Pearson, 1991; Rabalais et al., 2010), an oxic zone from 0 to 81 m (349 – 9 µM O_2), a redox zone from 81 to 143 m (< 9 µM O_2) and an anoxic zone below 143 m with no detectable O_2 concentrations. Hydrogen sulfide concentrations (H_2S,

Figure 2B) build-up slightly between 93 and 127 m (3 – 17 µM H_2S) but show a stronger increase below that depth interval (max. 172 µM H_2S). The turbidity anomalies covered a depth interval of approx. 62 m (81 – 143 m), reflecting the redox zone and the subsequent transition to anoxic conditions (chemocline); Kamyshny et al., 2013. For the Gotland Deep it is known that O_2 and H_2S can co-occur at the redox zone (Labrenz et al., 2010). However, since O_2 concentrations were only measured until first detection of H_2S, the co-occurrence of O_2 and H_2S is not documented in our dataset. Assuming that the suboxic water layer is mirrored by the depth interval of turbidity anomalies (Kamyshny et al., 2013) the redox zone is positioned between 81 m and 143 m water depth (Figure 2B).

The methane profile (Figure 2B) revealed concentrations lower than 10 nM CH_4 in the surface water. Below 80 m water depth, the methane concentration increased with increasing water depth with a methane maximum of 1233 nM CH_4 in the bottom water at 223 m water depth. The stable carbon isotope ratios in the deep water body are characterized by relatively low $\delta^{13}C$ CH_4 values (-84 ‰ at 223 m water depth) and a continuous enrichment of ^{13}C CH_4 towards the redox zone with strongly increasing $\delta^{13}C$ CH_4 values between 90 and 80 m water depth ($\delta^{13}C$ CH_4 from -67 ‰ to -45 ‰). Above the redox zone the isotopic ratio shifted back to more negative values ($\delta^{13}C$ CH_4 from -45 ‰ to -68 ‰) and showed values at the sea surface that are close to atmospheric $\delta^{13}C$ ratios of methane (-47.6 ‰, http://www.esrl.noaa.gov/gmd/dv/iadv/) measured in the Baltic Sea.

Methane oxidation rates were measured in the oxic, suboxic and anoxic part of the water column. The major consumption of methane occurred in a depth interval between 80 and 130 m (Figure 2C). The highest rate was measured within the redox zone (0.12 nM d^{-1} at 90 m water depth) with a methane turnover time of 455 d (k = 0.0022 d^{-1}, Figure 4).

Expression of the *pmoA* gene was restricted to only one type I methanotroph in a depth interval from 85 to 125 m. Sequence analysis revealed a similarity of 100 % to an uncultured

bacterium named Uncultured GotDeep_pmoA1 (accession number KC188735), which was already detected earlier in the central Baltic Sea (Schmale et al., 2012). *pmoA* genes could not be detected in this study.

4.2 Landsort Deep

Water column data from the Landsort Deep display thermohaline stratification similar to that observed in the Gotland Deep (Figure 3A). The thermocline extended from 10 to 30 m water depth, and the halocline was located in a depth interval from 50 to 80 m. Apart from the tubidity signal in the surface water, a pronounced signal was present in a depth interval between approx. 91 and 130 m (Figure 3A). The oxic zone extended from 0 to 84 m (351 – 9 µM O_2; see classification section 4.1 above). Again following the assumption, that turbidity anomalies can be used as an indicator for the depth interval of O_2/H_2S transition zone (Kamyshny et al., 2013), the redox zone is positioned between 84 and 130 m water depth (Figure 3B). H_2S concentrations increased only slightly within the lower redox zone and remained relatively constant towards the sediment. The deep water revealed maximal H_2S concentrations of about 14 µM.

The methane concentration profile showed a strong enrichment close to the bottom (2935 µM CH_4 at 422 m), a pronounced methane gradient within the redox zone (from 80 to 124 m) and methane concentrations lower than 10 nM CH_4 in the surface water. At the redox zone, a sharp stable carbon isotopic shift was found between 99 and 85 m ($\delta^{13}C$ CH_4, from -71 ‰ to -20 ‰ in the upper part of the redox zone).

Methane oxidation was detected throughout the water column, whereby the major consumption of methane took place between 80 and 115 m water depth (Figure 3C). The

highest rate was measured within the redox zone (0.61 nM d^{-1} at 90 m water depth) with a methane turnover time of 127 d (k = 0.0079 d^{-1}, Figure 4).

As determined for the Gotland Deep, the expression of the *pmoA* gene was restricted to the Uncultured GotDeep_pmoA1 in a depth interval from 70 to 115 m (Figure 3C). *pmoA* genes were detected between 80 and 115 m water depth.

5 Discussion

Our physical, chemical and microbiological results (summarized in Table 1) show considerable differences between both deeps. In the following chapter, we will discuss the different factors controlling the fate of methane in the Landsort Deep (LD) and Gotland Deep (GD) based on data of the methane dynamics and the hydrodynamic situation.

5.1 Microbial methane consumption in the Gotland and Landsort Deep

5.1.1 Concentration and stable isotope pattern

The measured $\delta^{13}C$ CH_4 values (GD: -84 ‰, 223 m; LD: -71 ‰, 347 m) in the anoxic waters of both deeps are in the range of those which are representative for a biogenic origin of methane (Whiticar, 1999). This stable isotope signature is modified by microbial methane turnover in the overlain water column as this consumption impacts the concentration distribution of methane and its stable carbon isotope pattern (Whiticar, 1999; Reeburgh, 2007; Schmale et al., 2010). Our dataset points to prominent microbial methane consumption within the redox zones in both deeps (Figure 2 and 3). The significance of this specific depth interval is emphasized by a constant methane concentration decrease and a pronounced change of the $\delta^{13}C$ CH_4 values. Here, the observed enrichment of ^{13}C CH_4 within the redox zone in both

deeps can be explained by isotopic discrimination during microbial methane oxidation due to the kinetic isotope effect that leads to an enrichment of ^{13}C CH_4 in the residual methane pool (Whiticar, 1999). In the LD, the steeper methane gradient within the redox zone together with the stronger ^{13}C CH_4 enrichment in the lower oxic zone indicates more pronounced and efficient methane consumption compared to the GD assuming similar Eddy diffusion.

5.1.2 Methane oxidation rates

The outstanding position of the redox zone in the LD and GD as an important depth interval for microbial methane oxidation is also supported by measured elevated oxidation rates in this specific depth. However, remarkable differences are obvious between both deeps. Compared to the redox zone of the LD, which is characterized by the highest oxidation rates (max. rate 0.61 nM d^{-1}), the rates in the GD (max. rate 0.12 nM d^{-1}) were much lower. Oxidation rates measured in the suboxic zone of anoxic basins like the central Black Sea: 1×10^{-3} – 1.6 nM d^{-1} (Reeburgh et al., 1991; Durisch-Kaiser et al., 2005) or the Cariaco Trench: 0.4 – 0.8 nM d^{-1} (Scranton, 1988) are in the same order of magnitude as the data obtained in this study. Also the integrated oxidation rates (ir_{ox}) calculated for the depth interval along the redox zone of the LD (4.85 µmol d^{-1} m^{-2}, 84 – 130 m) is almost three times as high as the integrated rate in the GD (1.77 µmol d^{-1} m^{-2}, 81 – 143 m). At this zone the maximum turnover rate constant (k) calculated for the LD (0.0079 d^{-1}) is nearly four times as high as the constant in the GD (0.0022 d^{-1}, Figure 4). Assuming that the turnover rate constant is reflecting the population size of methanotrophic microorganisms (Kessler et al., 2011), the growth of these organisms is maybe stimulated by the stronger stability of the intermediate water body that is less perturbed by lateral intrusions in the LD compared to the GD (see section 5.2.2). Furthermore, elevated turnover rate constants were also detected in the oxic zone of the LD and not only within the redox zone as it was observed in the GD. This is in accordance with the transcript

analysis which could confirm the expression of the *pmoA* gene above the redox zone of the LD, indicating active methanotrophs also in the oxic zone.

In addition to these perturbations, the concentration of methane also influences the abundance of the microorganisms involved in the turnover of CH_4 within the redox zones of both deeps. Previous studies showed that increased substrate availability results in a dynamic adaption of the population size of the aerobic methanotrophic community (Valentine et al., 2001; Kessler et al., 2011). In conjunction with our study, this would imply that in comparison to the GD the higher methane concentrations within the redox zone of the LD (GD: 200 nM CH_4, 139 m and LD: 799 nM CH_4, 124 m) promote microbial methane oxidation and the growth of the methanotrophic community. The different population sizes within the redox zones are also supported by our DNA analysis. In contrast to the GD where no *pmoA* genes could be amplified in PCR reaction and thus probably were below the detection limit, DNA analysis for the identification of *pmoA* genes on the samples obtained in the LD yielded in PCR products. Thus, the *pmoA* gene copy number at GD was below the detection limit of our approach. Within this study we were not able to determine this limit directly. But for soil methanotrophs it ranged between 10^1 and 10^2 copies of the *pmoA* gene per reaction (Kolb et al., 2003), which could be a realistic number also for our study.

To determine the kinetic fractionation factor (α) of microbial methane oxidation within the redox zones we created a plot of $\delta^{13}C$ CH_4 versus $1/CH_4$ (Figure 5) according to (Mau et al., 2012). To avoid any side effects in these calculations which could be caused by lateral intrusions (i.e. input of CH_4 from other regions with a different $\delta^{13}C$ CH_4 signature), we used in a first step the dataset obtained in the LD which is compared to the GD characterized by a less disturbed intermediate water layer (Dellwig et al., 2012). Motivated by the apparent restriction of methane oxidation within the redox zone, as observable from the methane concentration gradient and ^{13}C CH_4 enrichment in the LD redox zone (Figure 3B), we applied

a closed system Rayleigh fractionation approach (Coleman et al., 1981). The methane oxidation trend between the deep water (1192 nM CH_4, $\delta^{13}C$ -71 ‰) and the water depth which is characterized by the strongest ^{13}C CH_4 enrichment within the redox zone ($\delta^{13}C$ CH_4: -20 ‰ at 85 m water depth) fitted best with a fractionation factor (α) of 1.012 (Figure 5A). In a second step, we used this derived α to calculate the oxidation trend in the GD, which is characterized by a more disturbed intermediate water layer (Dellwig et al., 2012). The assumption of a similar α is justified because of comparable temperatures and chemical conditions, and in particular by the identification of the same single methanotrophic bacterium in both deeps (see section 5.1.3). The calculated theoretical oxidation trend can be used to classify each CH_4 data point into three main groups: below the mixing line (CH_4 affected by mixing processes), between the mixing line and oxidation trend (CH_4 influenced by mixing and partly influenced by oxidation) and above the oxidation trend (CH_4 clearly related to oxidation processes). Our results show that the CH_4 data points in both basins fit reasonably well in the ^{13}C CH_4 depleted part of the oxidation trend. However, within the redox zone of the eastern Gotland Basin a deviation is visible in the ^{13}C CH_4 enriched part (Figure 5B). Based on oceanographic studies, which indicated a stronger perturbation of the redox zone in the eastern compared to the western Gotland Basin (Dellwig et al., 2012; Kamyshny et al., 2013), we assume that the observed deviation from the oxidation trend results from enhanced mixing within the redox zone of the eastern Gotland Basin.

5.1.3 Aerobic methanotrophs in the redox zone

Sequence analysis revealed that in both deeps methane oxidation in the redox zone is restricted to type I methanotrophic bacteria indicating that the different environmental settings (i.e. methane concentrations and disturbances within the redox zone by lateral intrusions) did not influence the microbial diversity of aerobic methanotrophs. The exclusive detection of

type I methanotrophs confirms recently published biomarker analysis which indicate the absence of type II methanotrophic bacteria in the water column of the GD (Schmale et al., 2012; Berndmeyer et al., 2013). The restricted diversity of type I methanotrophs in the central Baltic Sea is in agreement with studies conducted by Schubert et al. (2006c) in the Black Sea, who identified type I methanotrophic bacteria as the most important methane consumer in the redox zone zone. However, other studies conducted in the oxic zone as well as in the redox zone of the Black Sea also proved the existence of type II and X methanotrophs (Durisch-Kaiser et al., 2005; Blumenberg et al., 2007). The methanotrophic bacteria identified in the GD and LD is restricted to the phylotype Uncultured GotDeep_pmoA1 (Schmale et al., 2012). A phylogenetically affiliated phylotype of the Uncultured GotDeep_pmoA1 was also detected in a meromictic crater lake (Lake Pavin) which is characterized by a permanently stratified water column (Biderre-Petit et al., 2011). Apart from the identified phylotype in the present study, two main phylotypes of type I methanotrophs have been found in the meromictic lake. We assume that the reduced diversity in the Baltic Sea redox zone is related to an overlap of sulfide- and oxygen-containing waters as a result of lateral intrusions (Dellwig et al., 2012). The influence of sulfide containing waters on the microbial diversity has been shown by (Labrenz et al., 2010). Based on this relation it is assumed that the toxicity of sulfide to many organisms may inhibit the activity of other methanotrophs than the detected phylotype (Schmale et al., 2012). However, a higher diversity of active aerobic methanotrophic bacteria in the compared to the GD less disturbed redox zone of the LD could not be detected.

The detection of the *mcrA* gene for analyzing anaerobic methanotrophs was not performed in our studies due to the main focus on aerobic methane oxidation. From a theoretical point of view, sulfate-depending methane oxidation (AOM) in the anoxic water layer should be possible as the ambient sulfate concentrations (LD 0.81 g kg^{-1} and GD 0.93 g kg^{-1}; derived from the averaged salinity in the anoxic water layer; calculated after Bruland, 1983) would

enable this process (Reeburgh, 2007). This assumption is supported by our methane oxidation rate measurements which indicate anaerobic turnover of methane in both basins. However, the determined oxidation rates are significantly affected by high standard deviations and a potential underestimation due to the chosen $^{14}CH_4$ tracer amount. The method developed for this study was designed to analyze microbial methane oxidation within the oxic and redox zone, so that these oxidation rates cannot provide a clear evidence for the existence of AOM processes.

5.2 Hydrodynamic controls on the fate of methane in the Gotland and Landsort Deep

5.2.1 Vertical mixing

The vertical transport of matter (e.g. nutrients, gases, particles) in the central Baltic Sea is strongly influenced by vertical mixing processes. The different intensities of mixing directly impact the concentration distribution pattern of chemical species in the water column (Nausch et al., 2008; Holtermann et al., 2012). Especially the transport across the chemocline influence important biogeochemical processes as reduced and energy-rich chemical species like CH_4, H_2S, iron (Fe^{2+}) and manganese (Mn^{2+}) are abundant in high concentrations within the deep water and can drive microbial reactions at the redox zone (Labrenz et al., 2005; Dellwig et al., 2012; Schmale et al., 2012).

Between 300 m water depth and the lower edge of the redox zone (130 m) the LD is characterized by a uniform methane profile whereas the methane concentrations in the GD decrease constantly with decreasing depth. The same relationship is also reflected by the H_2S profiles and the $\delta^{13}C$ CH_4 distribution in the anoxic water bodies. The shapes of the methane profiles are related to the different vertical mixing rates (K_ρ, see also Eq. 4) between the two basins, which are increased nearly 6 times in the LD compare to the GD (K_ρ: GD $1.1*10^{-5}$ m^2 s^{-1}, LD $6.2*10^{-5}$ m^2 s^{-1}, annual mean at 150 m water depth (Axell, 1998). The uniform shape

of the LD methane profile in a depth range between approx. 150 m and 300 m as well as the increase towards the bottom can be nicely explained by the vertical structure of K_ρ, which shows a maximum (K_ρ: 9.5*10^{-5} m^2 s^{-1}) in the depth range between 200 and 300 m and a decrease (K_ρ: 1.0*10^{-5} m^2 s^{-1}) to the bottom.

Assuming that the flux of methane from the anoxic deep water to the redox zone and the consumption of methane within the redox zone are in steady state, we can use our dataset to calculate vertical mixing rates (K_ρ) for the upper anoxic zone (GD: 143-200 m, LD: 130-250 m). Using the integrated methane oxidation rates (ir_{ox}) in the redox zones (see section 5.1.2) and the methane concentration gradients within the upper anoxic zone, K_ρ can be calculated according to Eq. (4), where c is the *in situ* concentration of methane [µmol m^{-3}] and z the water depth [m].

$$K_\rho = \frac{ir_{ox}}{dc/dz} \quad \left[m^2\, d^{-1}\right] \tag{4}$$

The mixing rates calculated by this method for the LD are one order of magnitude higher than those for the GD (GD: 2.5*10^{-6} m^2 s^{-1}, LD: 1.6*10^{-5} m^2 s^{-1}). This higher vertical mixing rate in the LD is in accordance with the observations of Axell (1998), who reported a 6 times larger K_ρ for the LD than for the GD at the 150 m depth level. However, the mixing rates calculated within the present study are 4 times lower compared to the values reported by Axell (1998). The enhanced vertical transport of methane implies a higher supply of substrate to the methanotrophic community within the redox zone of the LD.

5.2.2 Lateral intrusions

The turbidity in anoxic basins is often used as a marker to determine the depth of the chemocline. Turbidity anomalies near the chemocline reflect an incompletely understood phenomenon. It is often explained by the diffusion of reduced chemical species across the redox zone, which lead to the precipitation of metal oxides (e.g. oxides of Fe and Mn) or the oxidation of H_2S to elemental sulfur S^0 (Dellwig et al., 2010; Kamyshny et al., 2013). Another theory is that the energy-rich compounds transported from the anoxic zone across the chemocline increase microbial turnover of matter and thus the abundance of bacteria in a discrete depth interval (Prokhorenko et al., 1994; Dellwig et al., 2010; Labrenz et al., 2010). However, the distribution pattern can also be used to discuss the stability of that chemical boundary as lateral intrusions of external water masses into the redox zone will perturb the established chemical stratification (Kamyshny et al., 2013) and may inject O_2/H_2S enriched water into this specific depth interval (Dellwig et al., 2012). The turbidity profile of the GD (Figure 2A) reveals different distinct peaks along the redox zone. Previous studies in the GD indicate, that these turbidity anomalies are related to lateral intrusions into the redox zone (Lass et al., 2003; Dellwig et al., 2012). Therefore, lateral intrusions or internal waves produce perturbations in the intermediate water column and prevent the formation of a clearly defined redox zone. In contrast, the LD reveals only one pronounced turbidity signal on top of the redox zone with a constant decrease with increasing water depth (Figure 3A). Even if this decrease can currently not be explained, the clear trend without turbidity spikes (in contrast to the observation in the GD) point to a more undisturbed situation in the LD redox zone (Dellwig et al., 2012; Kamyshny et al., 2013). Temperature-salinity diagrams (T-S) are useful approaches to identify the strength of intrusions in the central Baltic Sea (Dellwig et al., 2012). Signatures of intrusions can be identified in the GD by slight variations in the T-S profiles across the entire redox zone (see insert Figure 6A). The LD is characterized by a relatively smooth T-S pattern indicating the undisturbed situation of this intermediate water layer (see insert Figure 6B).

6 Conclusions

In the present study, methanotrophic processes within the stratified water columns of the Gotland Deep and Landsort Deep (central Baltic Sea) were investigated to reveal their dependence on different hydrographic conditions. Within the redox zones of both deeps, microbial consumption of methane was identified by the distribution patterns of the concentration of methane, $^{13}C\ CH_4$, and elevated methane oxidation rates. In this intermediate depth interval one potentially active type I methanotrophic bacterium was identified at both sampling sites, indicating that the different hydrographic conditions apparently do not impact the diversity of methanotrophic communities. In contrast, the microbial turnover of methane in the redox zones reveals considerable differences with lower methane oxidation rates in the Gotland Deep compare to the Landsort Deep. The intensity of lateral intrusions and the vertical transport rate of methane from the anoxic zone into the redox zone are different between both deeps, and seem to represent the key-processes which control the turnover of methane within the redox zone. Our results confirm that pelagic microbial methane oxidation within redox gradients represent an efficient methane sink that prevents the escape of methane from the deep anoxic zone into the atmosphere. The comparative investigations in the Gotland Deep and Landsort Deep also indicate that this microbially mediated process can react on different environmental conditions by adapting the population size of methanotrophs and/or the rate of methane oxidation. Open questions regarding the involvement of other electron acceptors beside oxygen, the temporal dynamic of methane degradation as well as the verification of anaerobic methane oxidation in the deep anoxic waters need to be clarified in further studies.

Acknowledgements

Many thanks to the captain and the crew of R/V *Elisabeth Mann Borgese* for their support on cruise 06EZ/12/13. We would like to thank Tina Treude for the $^{14}CH_4$ tracer preparation and for her support during the establishment of the labeling experiments at the IOW. We thank Iris Liskow for the technical assistance to install the combustion line and Stine Kedzior for sample measuring. We further thank Birgit Sadkowiak for oxygen and hydrogen sulfide analysis as well as Jan Donath for supplying bathymetric maps and CTD work. We gratefully acknowledge Peter Holtermann, Martin Blumenberg, Christine Berndmeyer and Volker Thiel for fruitful discussions during paper preparation. We also thank Thomas Pape and an anonymous reviewer for their comments and suggestions to improve the manuscript. This study was supported by the Deutsche Forschungsgemeinschaft (DFG) through the grant SCHM 2530/2-1.

References

Altschul, S. F., Gish, W., Miller, W., Myers, E. W., and Lipman, D. J.: Basic local alignment search tool, J. Mol. Biol., 215, 403-410, doi:10.1016/S0022-2836(05)80360-2, 1990.

Axell, L. B.: On the variability of Baltic Sea deepwater mixing, J. Geophys. Res.-Oceans, 103, 21667-21682, 1998.

Bange, H. W., Bartell, U. H., Rapsomanikis, S., and Andreae, M. O.: Methane in the Baltic and North Seas and a reassessment of the marine emission of methane, Global Biogeochem. Cy., 8, 465-480, 1994.

Beal, E. J., House, C. H., and Orphan, V. J.: Manganese- and Iron-Dependent Marine Methane Oxidation, Science, 325, 184-187, doi:10.1126/science.1169984, 2009.

Berndmeyer, C., Thiel, V., Schmale, O., and Blumenberg, M.: Biomarkers for aerobic methanotrophy in the water column of the stratified Gotland Deep (Baltic Sea), Org. Geochem., 55, 103-111, doi:10.1016/j.orggeochem.2012.11.010, 2013.

Berndt, M. E., Allen, D. E., and Seyfried, W. E.: Reduction of CO_2 during serpentinization of olivine at 300 °C and 500 bar, Geology, 24, 351-354, 1996.

Biderre-Petit, C., Jézéquel, D., Dugat-Bony, E., Lopes, F., Kuever, J., Borrel, G., Viollier, E., Fonty, G., and Peyret, P.: Identification of microbial communities involved in the methane cycle of a freshwater meromictic lake, FEMS Microbiol. Ecol., 77, 533-545, 10.1111/j.1574-6941.2011.01134.x, 2011.

Blumenberg, M., Seifert, R., and Michaelis, W.: Aerobic methanotrophy in the oxic-anoxic transition zone of the Black Sea water column, Org. Geochem., 2007.

Boetius, A., Ravenschlag, K., Schubert, C. J., Rickert, D., Widdel, F., Gieseke, A., Amann, R., Joergensen, B. B., Witte, U., and Pfannkuche, O.: A marine microbial consortium apparently mediating anaerobic oxidation of methane, Nature, 407, 623-626, 2000.

Bourne, D. G., McDonald, I. R., and Murrell, J. C.: Comparison of *pmoA* PCR Primer Sets as Tools for Investigating Methanotroph Diversity in Three Danish Soils, Appl. Environ. Microbiol., 67, 3802-3809, 2001.

Brettar, I., and Rheinheimer, G.: Influence of carbon availability on denitrification in the central Baltic Sea, Limnol. Oceanogr., 37, 1146-1163, 1992.

Bruland, K.: Trace Elements in Sea Water, in: Chemical Oceanography, edited by: Riley, J. P., and Chester, R., Academic Press, London, 147-220, 1983.

Coleman, D. D., Risatti, J. B., and Schoell, M.: Fractionation of carbon and hydrogen isotopes by methane-oxidizing bacteria, Geochim. Cosmochim. Ac., 45, 1033-1037, doi:10.1016/0016-7037(81)90129-0, 1981.

Costello, A. M., and Lidstrom, M. E.: Molecular characterization of fuctional and phylogenetic genes from natural populations pf methanotrophs in lake sediments, Appl. Environ. Microbiol., 65, 5066-5074, 1999.

Dellwig, O., Leipe, T., März, C., Glockzin, M., Pollehne, F., Schnetger, B., Yakushev, E. V., Böttcher, M. E., and Brumsack, H.-J.: A new particulate Mn-Fe-P-shuttle at the redoxcline of anoxic basins, Geochim. Cosmochim. Ac., 74, 7100-7115, 2010.

Dellwig, O., Schnetger, B., Brumsack, H.-J., Grossart, H.-P., and Umlauf, L.: Dissolved reactive manganese at pelagic redoxclines (part II): Hydrodynamic conditions for accumulation, J. Marine Syst., 90, 31-41, 2012.

Durisch-Kaiser, E., Klauser, L., Wehrli, B., and Schubert, C.: Evidence of intense archaeal and bacterial methanotrophic activity in the Black Sea water column, Appl. Environ. Microbiol., 71, 8099-8106, 2005.

Dzyuban, A. N., Krylova, I. N., and Kuznetsova, I. A.: Properties of Bacteria Distribution and Gas Regime within the water Column of the Baltic Sea in winter, Oceanology+, 39, 348-351, 1999.

Ettwig, K. F., Butler, M. K., Le Paslier, D., Pelletier, E., Mangenot, S., Kuypers, M. M. M., Schreiber, F., Dutilh, B. E., Zedelius, J., de Beer, D., Gloerich, J., Wessels, H. J. C. T., van Alen, T., Luesken, F., Wu, M. L., van de Pas-Schoonen, K. T., Op den Camp, H. J. M., Janssen-Megens, E. M., Francoijs, K.-J.,

Stunnenberg, H., Weissenbach, J., Jetten, M. S. M., and Strous, M.: Nitrite-driven anaerobic methane oxidation by oxygenic bacteria, Nature, 464, 543-548, 2010.
Grasshoff, K., Ehrhardt, M., and Kremling, K.: Methods of seawater analysis, 3 ed., Verlag Chemie, Gulf Publishing Houston, 1999.
Gülzow, W., Rehder, G., Schneider v. Deimling, J., Seifert, T., and Tóth, Z.: One year of continuous measurements constraining methane emissions from the Baltic Sea to the atmosphere using a ship of opportunity, Biogeosciences, 10, 81-99, doi:10.5194/bg-10-81-2013, 2012.
Hallam, S. J., Girguis, P. R., Preston, C. M., Richardson, P. M., and DeLong, E. F.: Identification of Methyl Coenzyme M Reductase A (mcrA) Genes Associated with Methane-Oxidizing Archaea, Appl. Environ. Microb., 69, 5483-5491, doi:10.1128/aem.69.9.5483-5491.2003, 2003.
Holmes, A. J., Costello, A., Lidstrom, M. E., and Murrell, J. C.: Evidence that particulate methane monooxygenase and ammonia monooxygenase may be evolutionarily related, FEMS Microbiol. Lett., 132, 203-208, doi:10.1111/j.1574-6968.1995.tb07834.x, 1995.
Holtermann, P. L., Umlauf, L., Tanhua, T., Schmale, O., Rehder, G., and Waniek, J. J.: The Baltic Sea Tracer Release Experiment: 1. Mixing rates, J. Geophys. Res., 117, C01021, doi:10.1029/2011jc007439, 2012.
Kamyshny, A., Jr., Yakushev, E. V., Jost, G., and Podymov, O. I.: Role of Sulfide Oxidation Intermediates in the Redox Balance of the Oxic–Anoxic Interface of the Gotland Deep, Baltic Sea, in: Chemical Structure of Pelagic Redox Interfaces, edited by: Yakushev, E. V., The Handbook of Environmental Chemistry, Springer Berlin Heidelberg, 95-119, 2013.
Keir, R., Schmale, O., Seifert, R., and Sültenfuß, J.: Isotope fractionation and mixing in methane plumes from the Logatchev hydrothermal field, Geochem. Geophy. Geosy., 10, Q05005, doi:10.1029/2009GC002403, 2009.
Keir, R. S., Schmale, O., Walter, M., Sültenfuß, J., Seifert, R., and Rhein, M.: Flux and dispersion of gases from the "Drachenschlund" hydrothermal vent at 8°18' S, 13°30' W on the Mid-Atlantic Ridge, Earth Planet Sc. Lett., 270, 338-348, 2008.
Kessler, J. D., Valentine, D. L., Redmond, M. C., Du, M., Chan, E. W., Mendes, S. D., Quiroz, E. W., Villanueva, C. J., Shusta, S. S., Werra, L. M., Yvon-Lewis, S. A., and Weber, T. C.: A Persistent Oxygen Anomaly Reveals the Fate of Spilled Methane in the Deep Gulf of Mexico, Science, 331, 312-315, doi:10.1126/science.1199697, 2011.
Knittel, K., and Boetius, A.: Anaerobic Oxidation of Methane: Progress with an Unknown Process, Annu. Rev. Microbiol., 63, 311-334, 2009.
Kolb, S., Knief, C., Stubner, S., and Conrad, R.: Quantitative Detection of Methanotrophs in Soil by Novel pmoA-Targeted Real-Time PCR Assays, App. Environ. Microb., 69, 2423-2429, 10.1128/aem.69.5.2423-2429.2003, 2003.
Labrenz, M., Jost, G., Pohl, C., Beckmann, S., Martens-Habbena, W., and Jurgens, K.: Impact of Different In Vitro Electron Donor/Acceptor Conditions on Potential Chemolithoautotrophic Communities from Marine Pelagic Redoxclines, Appl. Environ. Microbiol., 71, 6664-6672, doi:10.1128/aem.71.11.6664-6672.2005, 2005.
Labrenz, M., Sintes, E., Toetzke, F., Zumsteg, A., Herndl, G. J., Seidler, M., and Jürgens, K.: Relevance of a crenarchaeotal subcluster related to Candidatus Nitrosopumilus maritimus to ammonia oxidation in the suboxic zone of the central Baltic Sea, ISME J., 4, 1496-1508, 2010.
Lass, H. U., Prandke, H., and Liljebladh, B.: Dissipation in the Baltic proper during winter stratification, J. Geophys. Res., 108, 3187, doi:10.1029/2002jc001401, 2003.
Lass, H. U., and Matthäus, W.: General oceanography of the Baltic Sea, in: State and evolution of the Baltic Sea, 1952-2005, edited by: Feistel, R., Nausch, G., and Wasmund, N., John Wiley & Sons, Inc., New Jersey, 5-44, 2008.
Matthäus, W., Nehring, D., Feistel, R., Nausch, G., Mohrholz, V., and Lass, H. U.: The inflow of high saline water into the Baltic Sea, in: State and evolution of the Baltic Sea, 1952-2005, edited by: Feistel, R., Nausch, G., and Wasmund, N., John Wiley & Sons, Inc., New Jersey, 265-310, 2008.

Mau, S., Rehder, G., Sahling, H., Schleicher, T., and Linke, P.: Seepage of methane at Jaco Scar, a slide caused by seamount subduction offshore Costa Rica, Int J Earth Sci (Geol Rundsch), 1-15, doi:10.1007/s00531-012-0822-z, 2012.
McDonald, I. R., Bodrossy, L., Chen, Y., and Murrell, J. C.: Molecular Ecology Techniques for the Study of Aerobic Methanotrophs, Appl. Environ. Microbiol., 74, 1305-1315, doi:10.1128/aem.02233-07, 2008.
Michaelis, W., Gerhard, B., Jenisch, A., Ladage, S., Richnow, H. H., Seifert, R., and Stoffers, P.: Methane and ^{3}He anomalies related to submarine intraplate volcanic activities, Mitteilungen aus dem Geologisch-Paläontologischen Institut der Universität Hamburg, 69, 117-127, 1990.
Modin, O., Fukushi, K., and Yamamoto, K.: Denitrification with methane as external carbon source, Water Res., 41, 2726-2738, 2007.
Nausch, G., Nehring, D., and Nagel, K.: Nutrient concentrations, trends and their relation to eutrophication, in: State and evolution of the Baltic Sea, 1952-2005, edited by: Feistel, R., Nausch, G., and Wasmund, N., John Wiley & Sons, Inc., New Jersey, 337-366, 2008.
Prokhorenko, Y. A., Krasheninnikov, B. N., Agafonov, E. A., and Basharin, V. A.: Experimental studies of the deep turbid layer in the Black Sea, Phys. Oceanogr., 5, 133-139, 1994.
Rabalais, N. N., Diaz, R. J., Turner, R. E., Gilbert, D., and Zhang, J.: Dynamics and distribution of natural and human-caused hypoxia, Biogeosciences, 7, 585-619, 2010.
Reeburgh, W. S., Ward, B. B., Whalen, S. C., Sandbeck, K. A., Kilpatrick, K. A., and Kerkhof, L. J.: Black Sea methane geochemistry, Deep-Sea Res., 38, 1189-1210, 1991.
Reeburgh, W. S.: Ocean methane biogeochemistry, Chem. Rev., 107, 486-513, 2007.
Reissmann, J. H., Burchard, H., Feistel, R., Hagen, E., Lass, H. U., Mohrholz, V., Nausch, G., Umlauf, L., and Wieczorek, G.: Vertical mixing in the Baltic Sea and consequences for eutrophication - A review, Progr. Oceanogr., 82, 47-80, 2009.
Schmale, O., Schneider von Deimling, J., Gülzow, W., Nausch, G., Waniek, J. J., and Rehder, G.: Distribution of methane in the water column of the Baltic Sea, Geophys. Res. Lett., 37, L12604, doi:10.1029/2010gl043115, 2010.
Schmale, O., Blumenberg, M., Kießlich, K., Jakobs, G., Berndmeyer, C., Labrenz, M., Thiel, V., and Rehder, G.: Aerobic methanotrophy within the pelagic redox-zone of the Gotland Deep (central Baltic Sea), Biogeosciences, 9, 4969-4977, doi:10.5194/bg-9-4969-2012, 2012.
Schubert, C. J., Coolen, M. J. L., Neretin, L. N., Schippers, A., Abbas, B., Durisch-Kaiser, E., Wehrli, B., Hopmans, E. C., Sinninghe Damsté, J. S., Wakeham, S., and Kuypers, M. M. M.: Aerobic and anaerobic methanotrophs in the Black Sea water column, Environ. Microbiol., 8, 1844-1856, 2006a.
Schubert, C. J., Durisch-Kaiser, E., Holzner, C. P., Klauser, L., Wehrli, B., Schmale, O., Greinert, J., McGinnis, D., De Batist, M., and Kipfer, R.: Methanotrophic microbial communities associated with bubble plumes above gas seeps in the Black Sea, Geochem. Geophy. Geosy., 7, doi: 10.1029/2005GC001049, 2006b.
Schubert, C. J., Durisch-Kaiser, E., Klauser, L., Vazquez, F., Wehrli, B., Holzner, C. P., Kipfer, R., Schmale, O., Greinert, J., and Kuypers, M. M. M.: Recent studies on sources and sinks of methane in the Black Sea, in: Past and present water column anoxia, IV. Earth and Environmental Sciences ed., edited by: Neretin, L. N., NATO Science Series, Springer, Netherlands, 419-441, 2006c.
Scranton, M. I.: Temporal variations in the methane content of the Cariaco Trench, Deep-Sea Res., 35, 1511-1523, doi:10.1016/0198-0149(88)90100-8, 1988.
Segers, R.: Methane production and methane consumption: a review of processes underlying wetland methane fluxes, Biogeochemistry, 41, 23-51, doi:10.1023/A:1005929032764, 1998.
Thomas, S.: Vergleich und Optimierung analytischer Methoden zur Bestimmung des Methangehalts in Seewasser, Diplomarbeit, Universität Rostock, 2011.
Treude, T., Boetius, A., Knittel, K., Wallmann, K., and Barker Joergensen, B.: Anaerobic oxidation of methane above gas hydrates at Hydrate Ridge, NE Pacific Ocean, Mar. Ecol.-Prog. Ser., 264, 1-14, 2003.

Treude, T., Krüger, M., Boetius, A., and Jørgensen, B. B.: Environmental control on anaerobic oxidation of methane in the gassy sediments of Eckernförde Bay (German Baltic), Limnol. Oceanogr., 1771-1786, 2005.
Tyson, R. V., and Pearson, T. H.: Modern and ancient continental shelf anoxia: an overview, Geological Society, London, Special Publications, 58, 1-24, doi:10.1144/gsl.sp.1991.058.01.01, 1991.
Valentine, D. L., and Reeburgh, W. S.: New perspectives on anaerobic methane oxidation, Environ. Microbiol., 2, 477-484, 2000.
Valentine, D. L., Blanton, D. C., Reeburgh, W. S., and Kastner, M.: Water column methane oxidation adjacent to an area of active hydrate dissociation, El River Basin, Geochim. Cosmochim. Ac., 65, 2633-2640, 2001.
Weinbauer, M. G., Fritz, I., Wenderoth, D. F., and Höfle, M. G.: Simultaneous extraction from bacterioplankton of total RNA and DNA suitable for quantitative structure and functional analyses, Appl. Environ. Micobiol., 68, 1082-1084, 2002.
Whiticar, M. J.: Carbon and hydrogen isotope systematics of bacterial formation and oxidation of methane, Chem. Geol., 161, 291-314, 1999.
Wuebbles, D. J., and Hayhoe, K.: Atmospheric methane and global change, Earth-Sci. Rev., 57, 177-210, doi:10.1016/S0012-8252(01)00062-9, 2002.

Table 1. Result summary

Parameter	Gotland Deep	Landsort Deep
depth interval of the redox zone	81 – 143 m	84 – 130 m
$\delta^{13}C$ CH_4 (redox zone)	-60 – -79 ‰	-20 – -72 ‰
max. CH_4 conc. (bottom water)	1233 nM, 223 m	2935 nM, 422 m
$\delta^{13}C$ CH_4 (bottom water)	-84 ‰, 223 m	-71 ‰, 422 m
max. methane oxidation rate (r_{ox})	0.12 nM d^{-1}, 90 m	0.61 nM d^{-1}, 90 m
max. turnover rate constant (k)	0.0022 d^{-1}	0.0079 d^{-1}
min. methane turnover time ($1/k$)	455 d	127 d
integrated methane oxidation rates in the redox zone (ir_{ox})	1.77 µmol d^{-1} m^{-2}	4.85 µmol d^{-1} m^{-2}
vertical mixing rates (K_p, upper anoxic zone)	$2.5*10^{-6}$ m^2 s^{-1}	$1.6*10^{-5}$ m^2 s^{-1}
pmoA detection (DNA analysis)	not achieved	80 – 115 m
pmoA gene expression (mRNA analysis)	85 – 125 m	70 – 115 m

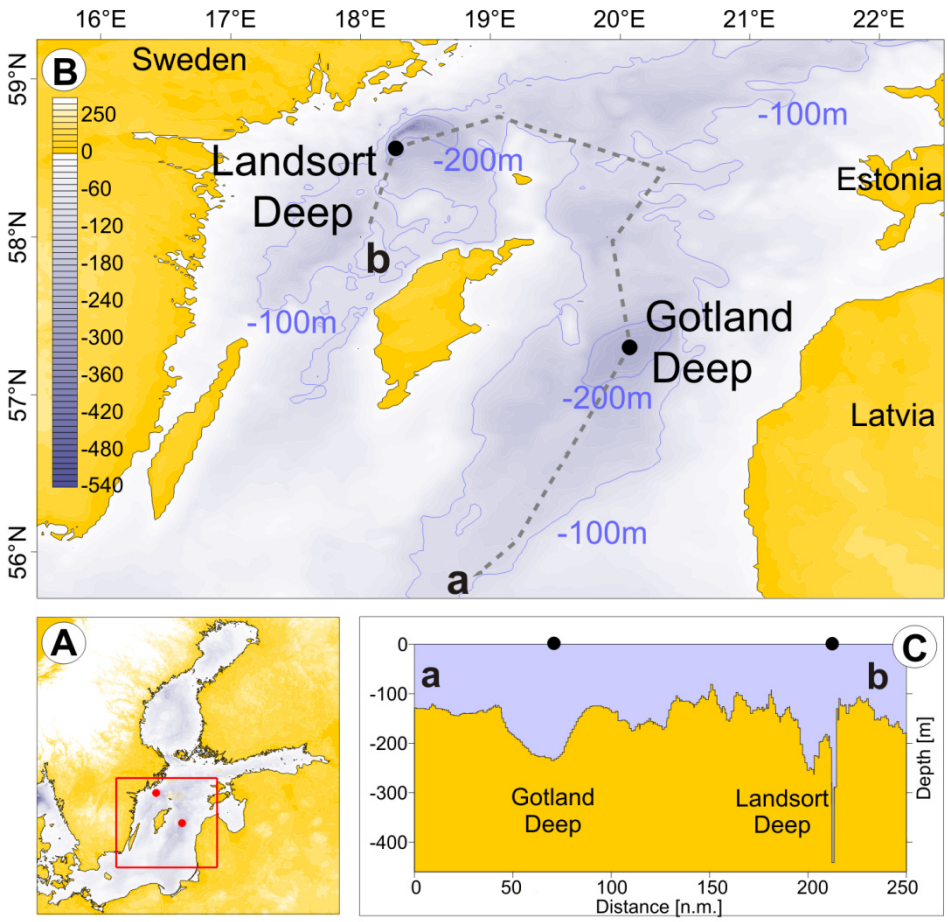

Figure 1. (**A**) Sampling sites in the central Baltic Sea (red dots). **(B)** Bathymetric map of the central Baltic Sea with the Gotland Deep in the eastern and the Landsort Deep in the western Gotland Basin. **(C)** Cross section from the eastern **(a)** to the western Gotland Basin **(b)**.

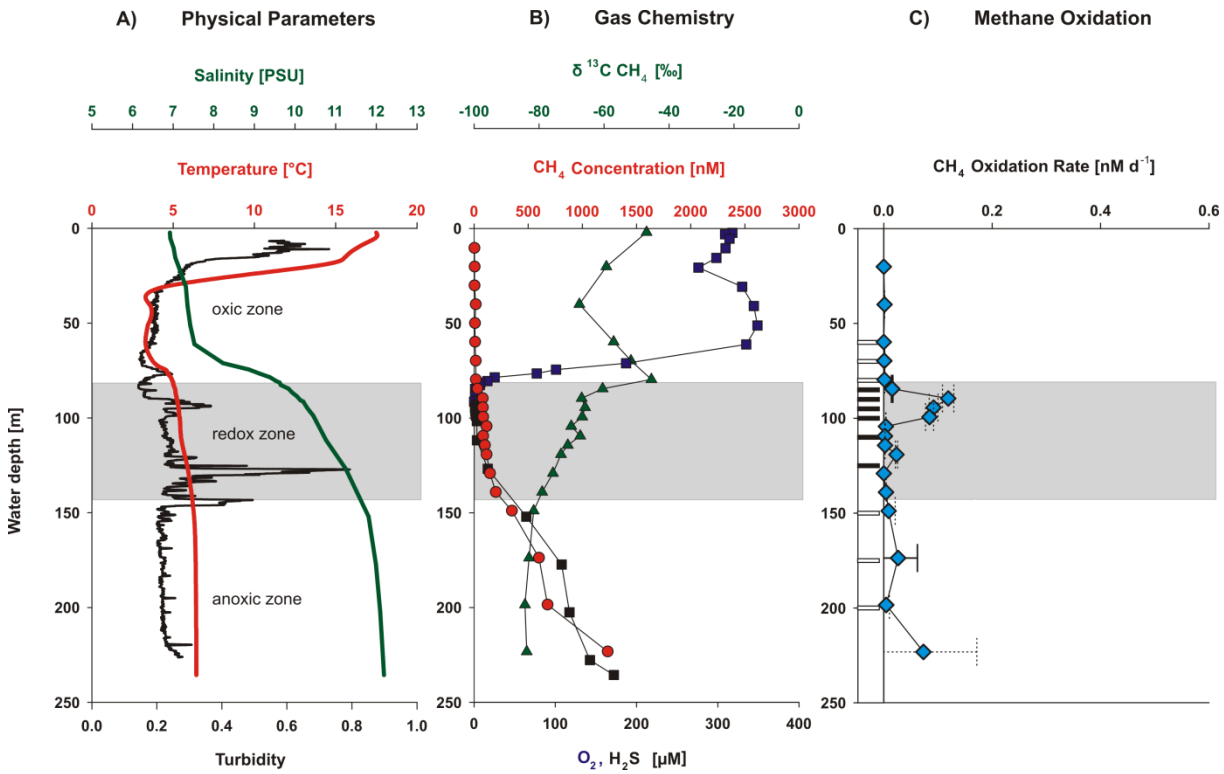

Figure 2. Gotland Deep. **(A)** Vertical profiles of salinity (green), temperature (red), and turbidity (black); **(B)** Oxygen (blue squares), hydrogen sulfide (black squares), methane (red circles), and $\delta^{13}C$ values of methane (green triangles); **(C)** Methane oxidation rates (light blue diamonds), and sampling depths of *pmoA* gene expression analysis (black bars denote the occurrence and white bars the absence of active type I methanotrophs). To obtain the standard deviation (*s*) for methane oxidation rates, triplicates were taken in three water depths (70, 85, 175 m). The solid error bars indicate the standard deviation from these triplicates whereas the dashed error bars show the standard deviation calculated from these triplicates for the single water samples. The redox zone is indicated by the gray shaded area.

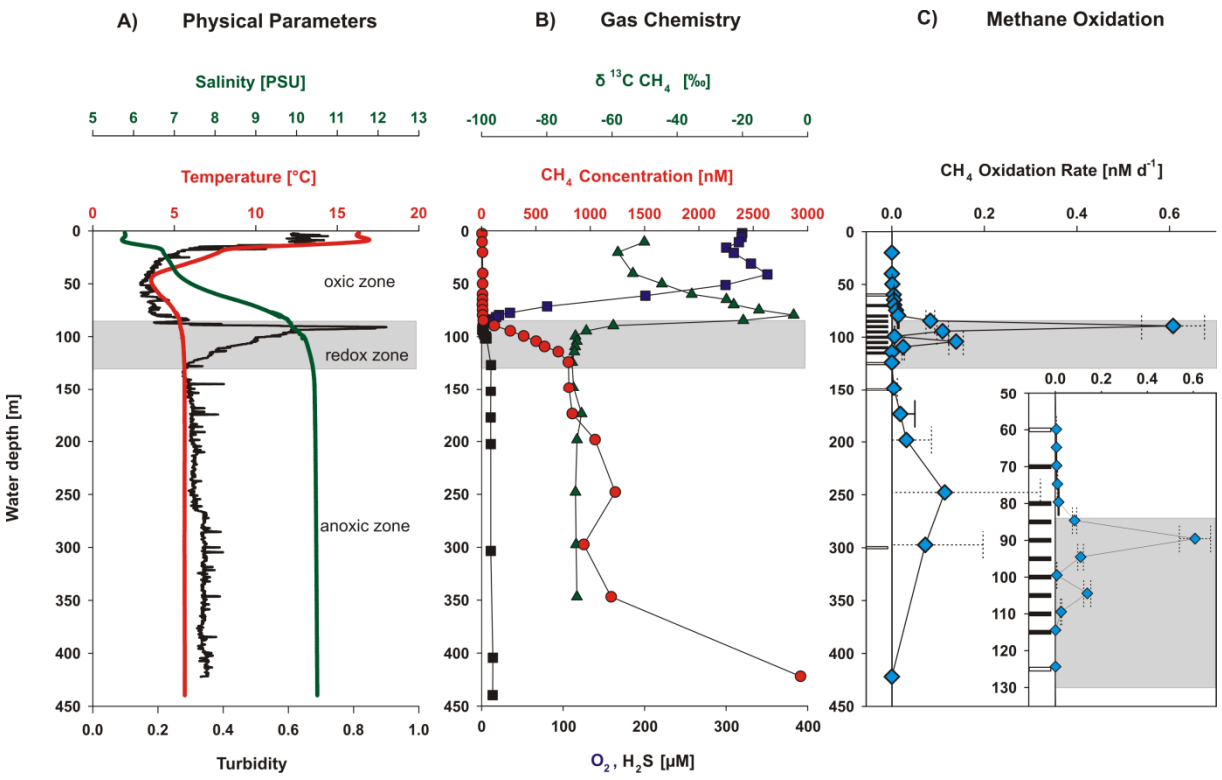

Figure 3. Landsort Deep. **(A)** Vertical profiles of salinity (green), temperature (red), and turbidity (black); **(B)** Oxygen (blue squares) and hydrogen sulfide (black squares), methane (red circles), and $\delta^{13}C$ values of methane (green triangles); **(C)** Methane oxidation rates (light blue diamonds), and sampling depths of *pmoA* gene expression analysis (black bars denote the occurrence and white bars the absence of active type I methanotrophs). To obtain the standard deviation (*s*) for methane oxidation rates, triplicates were taken in three water depths (70, 80, 175 m). The solid error bars indicate the standard deviation from these triplicates whereas the dashed error bars show the standard deviation calculated from these triplicates for the single water samples. The redox zone is indicated by the gray shaded area. The insert in **C)** illustrates the depth interval of the redox zone in higher vertical resolution.

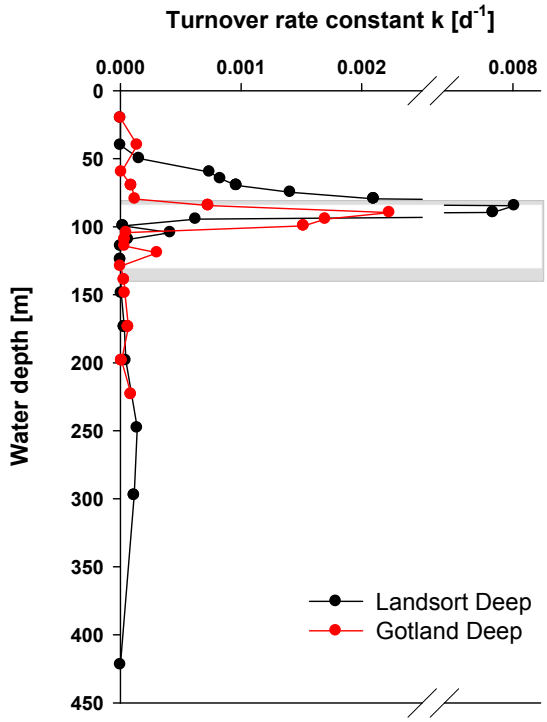

Figure 4. Turnover rate constants (*k*) from the Gotland Deep (red) and Landsort Deep (black). Indicated are the redox zones of the Gotland Deep (grey shaded area) and the Landsort Deep (white rectangle).

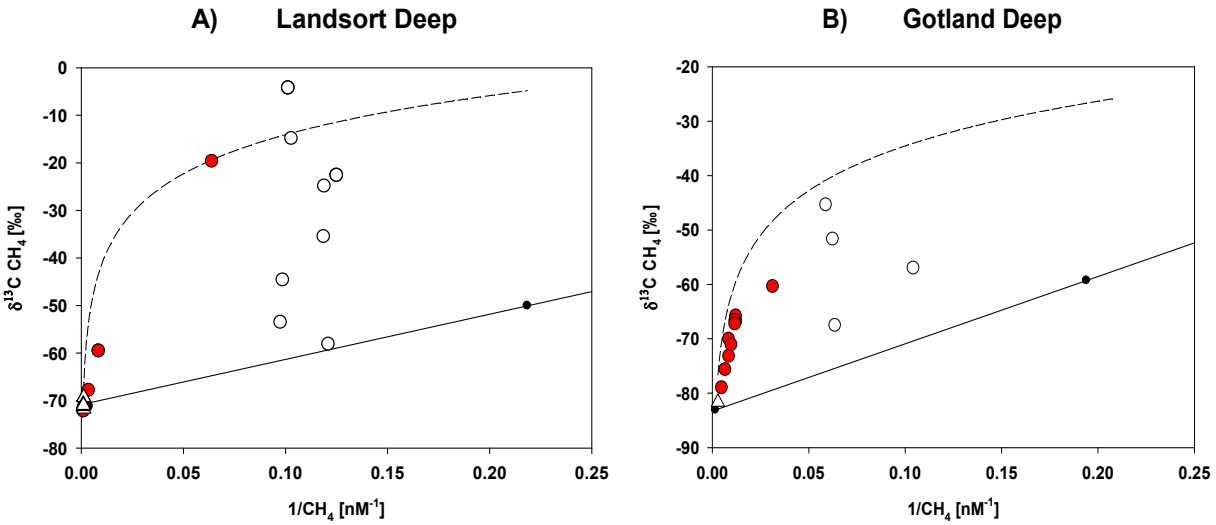

Figure 5. Landsort Deep **(A)** and Gotland Deep **(B)**. $\delta^{13}C$ CH_4 versus $1/CH_4$. Please note different scales for $\delta^{13}C$ CH_4. The solid lines denote mixing between deep and surface water, the dashed lines represent the oxidation trends based on a fractionation factor of $\alpha = 1.012$, the open triangles indicate the anoxic zone, the red circles the redox zone, and the open circles the oxic zone.

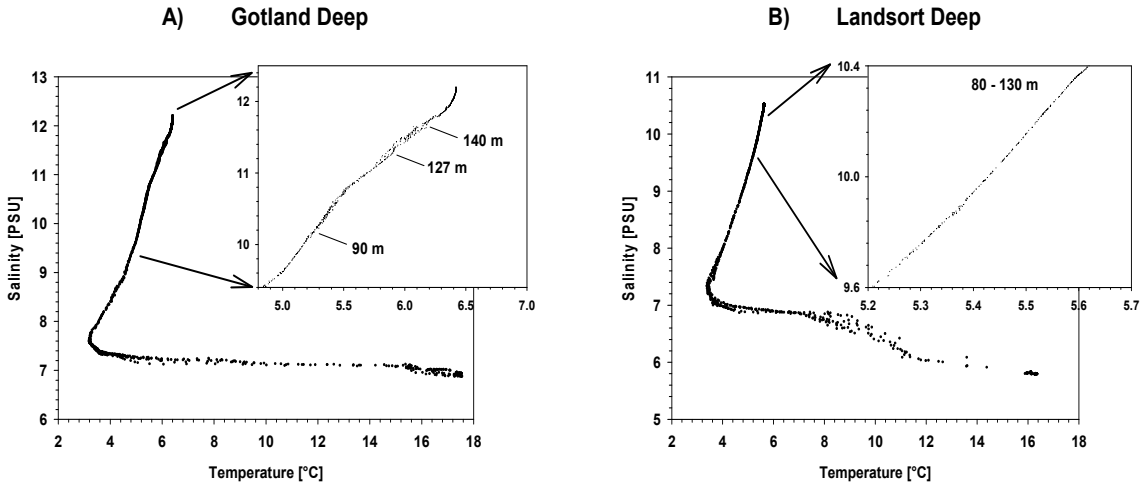

Figure 6. Temperature-salinity diagrams. The inserts denote the depth interval where the redox zone is located.